POWER FACTOR IMPROVEMENT AND DYNAMIC PERFORMANCE OF AN INDUCTION MACHINE WITH CONVERTER-FED ROTOR

V.Sindhuja [1] T.Ravali[2] MD.Imran Dr.M.Ramesh
[12]Student of B.Tech(EEE) Assistant Professor of EEE Professor & HOD of EEE
Imranmohannad5555@gmail.com marpuramesh223@gmail.com
Vaageswari College Of Engineering,Karimnagar

Abstract—This paper investigates an induction machine with a novel concept of the rotor fed by a converter. The stator is Y connected and directly connected to the grid, while the rotor windings are open-ended and fed by a back-to-back converter with a floating capacitor. Power factor and efficiency improvements of the induction motor are studied with different settings of phase-shift angle between the two converters. Moreover, the dynamic performance of the induction machine is explored in MATLAB/ Simulink and verified experimentally on a 1.8-kW induction machine in the laboratory. The result shows good agreement between simulation and experiment. At a constant speed, variable load operation of the induction machine is obtained by setting the frequency of the rotor voltage.

I. INTRODUCTION

The induction machine is widely used in industry because of its reliability, robustness and cost effectiveness. One inherent drawback of induction machines is that they draw reactive power from the grid and the power factor can be poor. Especially when the machine starts or operates with light loads, power factor and efficiency are drastically reduced [1]. Power factor improvement of induction machine is thus attractive and has been pursued for decades.

The simplest way to compensate the reactive power is to connect capacitor banks at the machine terminals. However, an unsuitable selection of capacitance may result in overvoltage due to self-excitation when the machine is disconnected from the supply, which could damage the machine [1]–[4]. This approach is not flexible since different capacitances are needed when the loading condition changes. A scheme of supplying variable capacitance is proposed in [5], where the induction machine is directly connected to the grid while a three phase pulse width modulation (PWM) converter with a floating capacitor is connected at the induction machine terminals. However, the improved power factor is realized only for the grid but not for the induction machine itself. The losses in the machine are not reduced thus the machine still suffers from poor power factor and hence poor efficiency.

In the 1980s, as an alternative to improve the mains power factor, the stator windings of a cage-rotor induction machine were rewound to achieve unity power factor [6], [7]. The stator windings were divided into two groups with different number of turns. The two sets of windings were electrically connected. This attracted a lot of interest at that time [8]. Different connections of two sets of identical stator windings are investigated in [9]. The results from [6], [9] both show that the mechanical output capability of the rewound induction machine is reduced compared with the original machine.

With the development of power electronics, topologies using rectifiers and inverters become interesting. In one of these topologies, a rectifier is connected to the grid and supplies a dc voltage to the PWM inverter connected to the stator of induction machine [10]. The power factor of the induction machine can be improved by regulating the PWM inverter output voltage to the stator windings. Furthermore, the rectifier can be replaced by a converter which enables the bidirectional power flow between the grid and induction machine thereby increasing the power factor. However, harmonics are introduced to the power network because of the switching power devices. A topology with a high frequency ac link between grid and machine side converters and other filters are investigated to reduce the current harmonics.

Instead of directly connecting the capacitors to the machine or the power network [1]–[4] to increase power factor and reduce harmonics, an extra set of stator winding is introduced to supply the required equivalent capacitance to the stator circuit. This is referred to as the dual stator winding induction machine. Two electrically isolated but magnetically coupled three-phase windings are installed in the stator in the mentioned induction machine. The two sets of windings can be designed to have the same or dissimilar pole and phase numbers. The main winding is connected to the grid while the auxiliary winding is connected to a three-phase PWM converter with a floating capacitor. Power factor improvement can be obtained by introducing a proper capacitance to the induction machine through the converter using a suitable modulation method. Alternatively, the auxiliary stator winding can be avoided and the three-phase converter is connected to the stator by accessing the Y-point of the stator windings. The converters in the above mentioned topologies need to be dimensioned for rated voltage to enable the machine to operate over the complete load range. Furthermore, the induction machine can be excited from the rotor side in the case of a wound rotor induction machine, such as the doubly-fed induction machines (DFIM).

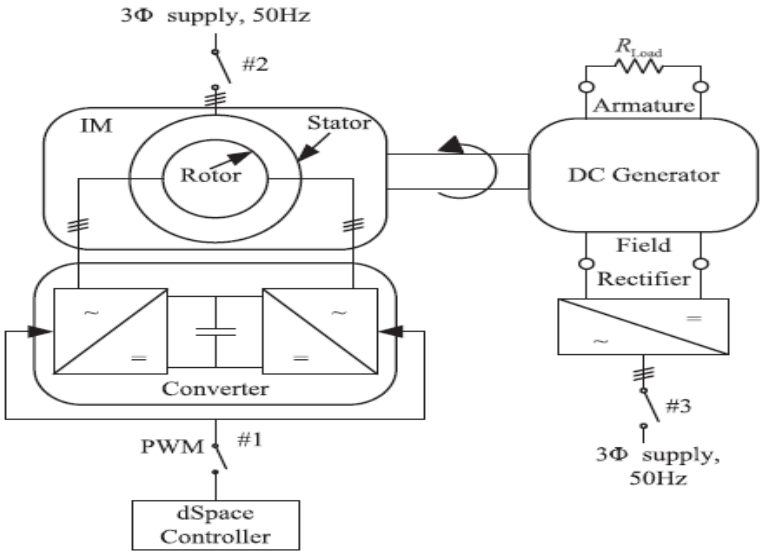

Fig:1. Configuration of the system.

Especially, unity power factor can be obtained within 25% to 100% of the rated mechanical power with the help of an external exciter sharing the back-to-back converter with the rotor of the induction machine. This topology is capable of controlling both active and reactive power, and consequently also the

power factor. However, power factor correction in DFIM requires closed loop control where the exact position of the flux vector is needed.

Another recent novel topology for power factor improvement is proposed in [27], in which a back-to-back converter with a floating capacitor is connected to the rotor windings. Power factor improvement can be achieved by magnetizing the machine from the rotor side with the reactive power supplied by the rotor-connected converter. It should be noted that, unlike the DFIM, the topology in [27] can only deal with the reactive power since the dc-link only contains a floating capacitor. However, the power factor will be improved automatically in this topology with open loop control. Specifically, the power factor of the induction machine at certain speed and load can be calculated with known machine parameters [28].

Studies on the topology proposed in [27] show that the stator power factor can be improved over a wide range of load torque. In this paper, the impact of changing the phase-shift angle between the two back-to-back connected converters on power factor improvement is further studied. Efficiency improvement for the induction machine as well as the whole system is also studied. Moreover, dynamic performance of the induction machine including starting, loading and load changing is investigated through simulation and experiment.

II. SYSTEM CONFIGURATION AND PRINCIPLE OF OPERATION

In the presented topology, shown in Fig. 1, the stator windings are Y-connected with the three phases directly connected to the grid.

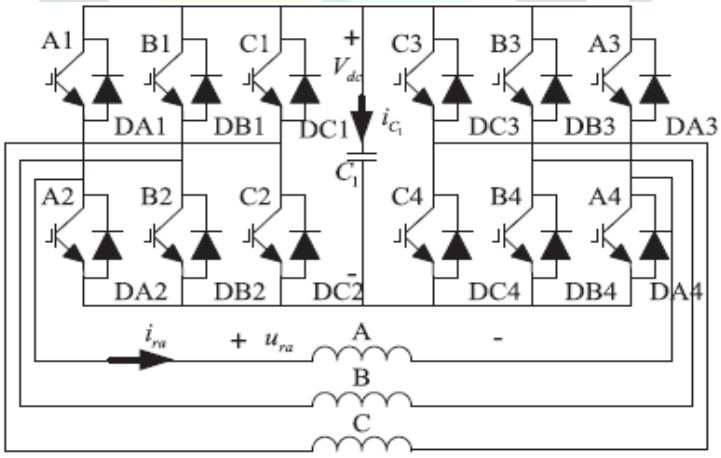

Fig:2. Connection of the back-to-back converter to the rotor windings.

Each of the three rotor phase windings are short-circuited via a back-to-back converter, as shown in Fig. 2. Hence, it is possible to magnetize the induction machine from the rotor side. The converter is connected to the rotor windings through sliprings and controlled by a dSpace controller box. The switching signals are divided into two groups, one for each converter. Sinusoidal SPWM strategy is applied to the two voltage source converters with the same switching frequency and modulation index. The phase-shift angle, θps, between the two converters can be varied from −180◦ to +180◦ [31]. A zero θps means that the rotor

windings are short-circuited. θps = ±180◦ means that full voltage is supplied. The dc-link voltage of the converter is not controlled but automatically balanced depending on the speed and load of the induction machine.

The operating of the system can be realized in three steps. Firstly, indicated by #1 in Fig. 1, the switching signals are sent to the 12 power electronic valves, for instance IGBTs in this paper, A1–A4, B1–B4 and C1–C4 shown in Fig. 2. The fundamental frequency of the switching signals can be expressed as

$$f_2 = \frac{n_s - n_r^*}{n_s} f_1 \quad \text{.....(1)}$$

where ns and n∗ r are the synchronous and reference speed respectively while f1 is the stator frequency. Secondly, indicated by #2 in Fig. 1, the stator is connected to a three-phase voltage supply and the machine is started at no load. The flux generated in the stator will induce ac currents in the rotor windings. In the beginning, even though the switching signals are available, the valves cannot conduct since the dc-link voltage is zero. These currents can only flow through the anti-paralleled diodes thereby charging the capacitor. The level of capacitor voltage will depend on the phase-shift angle θps between the two converters. If θps = 0◦, the capacitor cannot discharge through the IGBTs and its voltage will rise to a very high level. In contrast if θps = 180◦, the capacitor voltage will be low which however makes it difficult to magnetize the machine from the rotor side. In this paper θps = 60◦ is used during the start of the machine. In addition, the high starting rotor current will rapidly discharge the capacitor during the acceleration of the induction machine. Thus, the capacitor voltage cannot be maintained and the converter is unable to supply a voltage of constant frequency to the rotor windings.

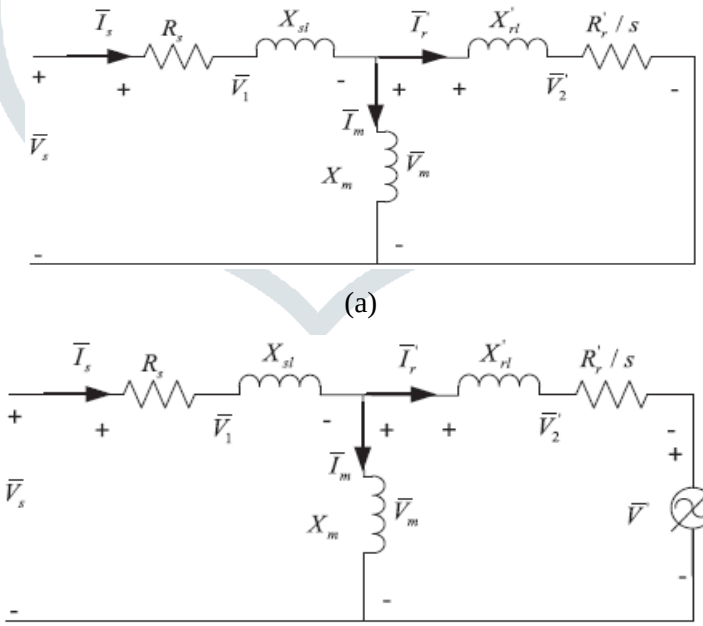

Fig:3. Equivalent circuit of the induction machine: (a) without rotor connected converter; (b) with rotor-connected converter.

As a result, the machine accelerates to the no load speed instead of the reference speed n∗ r . Once the machine stabilizes to its no-load steady-state speed, load torque is applied, indicated by #3 in Fig. 1. The capacitor will be charged to a certain voltage according to the applied load and then maintain stable. Thereafter the converter can provide a three-phase voltage with slip frequency of f2 to the rotor windings. Consequently the speed of the induction machine settles to n∗ r. The starting procedure described above is demonstrated in Section V where the dynamic performance of the system is investigated.

Moreover, the power factor of the induction machine can be improved in the presented topology, which will be illustrated in the following. By comparing the equivalent circuits and phasor diagrams of the induction machine without and with the rotor connected converter, shown in Figs. 3(a), 4(a) and 3(b), 4(b), respectively, it can be seen that the converter contributes to a voltage vector $\overline{V}_r$ in the rotor circuit. Furthermore, the voltage vector $\overline{V}_r$ will change the magnitude and phase angle of the rotor current vector $\overline{I}_r$, as seen in Fig. 4(b). As the rotor and the stator current vectors are related to each other, the phase angle of the stator current vector $\overline{I}_s$ will be shifted accordingly [27]. At steady state, the voltage vector $\overline{V}_r$ should lag the rotor current $\overline{I}_r$ by 90◦ since the dc-link is a capacitor, as is shown in Fig. 4(b). If under transient conditions $\overline{V}_r$ and $\overline{I}_r$ have an angle of α instead, as shown in Fig. 4(c), the rotor current component $\overline{I}_r \cos \alpha$ will charge or discharge the capacitor until it reaches steady state conditions with $\overline{V}_r$ lagging $\overline{I}_r$ by 90◦ [32]. Furthermore, the voltage $\overline{V}_2$ on the rotor winding cannot be changed lagging $\overline{V}_m$, as shown in Fig. 4(d). The phase angle relationship between $\overline{V}_r$ and $\overline{I}_r$ can never be satisfied in this case. The rotor current $\overline{I}_r$ as well as the stator current $\overline{I}_s$ can only be moved in the anti-clockwise direction, as shown in Fig. 4(b). It is therefore impossible to realise the phasor diagram shown in Fig. 4(d) where the power factor is reduced. Consequently, the power factor of the presented induction machine is always improved as shown in Fig. 4(b).

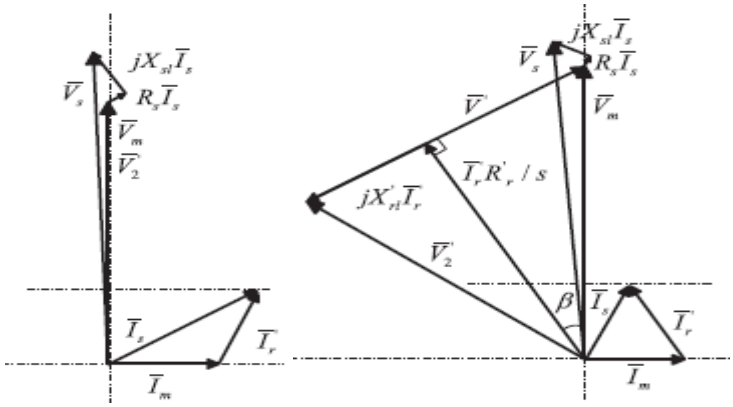

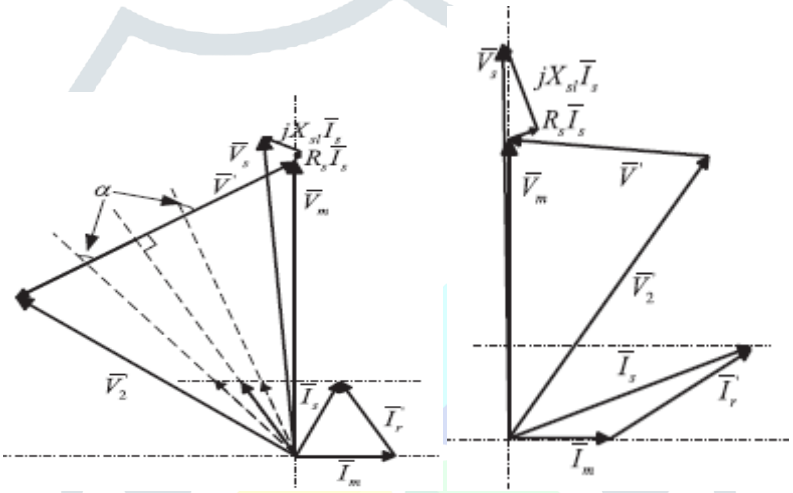

Fig:4. Phasor diagrams for motor operation: (a) for the conventional induction machine; (b) for an induction machine with the rotor windings connected to a converter; (c) for the case when ¯I_r is not perpendicular to ¯ V_; (d) for the case when ¯ V_2 in (b) is positioned incorrectly.

This topology is applicable to all induction machines with open-end rotor windings regardless of the power rating of the machine. Constant speed variable load operation is possible within a speed and load range that depends on the size, pole number and cooling of the machine. It is also possible to run the machine at low speed under light load conditions [28]. Moreover, this configuration has potential as a brushless topology if the converter together with the controller can be integrated in the rotor replacing the carbon brushes and slip-rings.

III. SIMULINK MODEL OF PROPOSED SYSTEM

The dynamic performance of the presented system is explored using MATLAB/Simulink. The machine specifications are given in Table. I. The Simulink model shown in Fig. 5 mainly consists of a wound rotor induction machine, a three-phase voltage source, a mechanical load source, two back to- back connected converters fed by a PWM generation block. As can be seen in Fig. 5, a resistor is paralleled with the dc-link capacitor. In reality this resistor is connected in the converter for the reason of safety to protect the capacitor from unwanted transients. It is also considered in simulation.

TABLE I
MACHINE SPECIFICATIONS (GIVEN IN INVERTED CONFIGURATION)

P_N (kW)	1.8	n_N (r/min)	1400
f_1 (Hz)	50	P.F.	0.8
U_{s1-l} (V)	180	U_{r1-l} (V)	380
I_s (A)	10	I_r (A)	4.5
R_s (Ω)	0.8	R_r (Ω)	2.15
X_{s1} (Ω)	1.076	X_{r1} (Ω)	4.796
N_s/N_r	180/380	X_m (Ω)	14.8

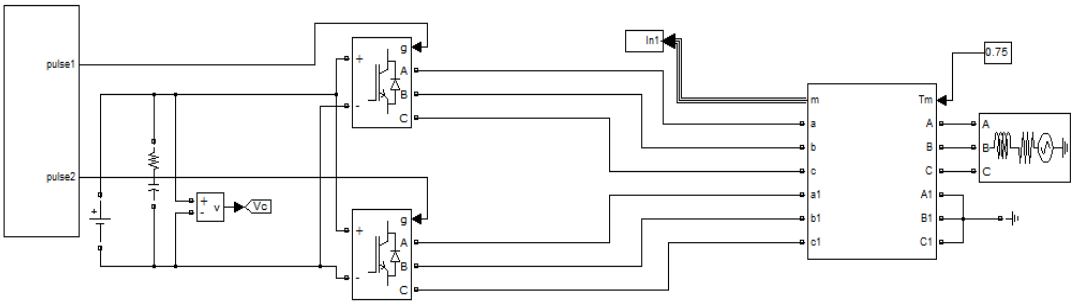

Fig:5. Simulink model.

It should be noted that the machine in the simulation is connected in inverted configuration, i.e., the rotor is connected to the grid while the stator is connected to the back-to-back converter. This is because the stator windings of the induction machine are open-ended while the rotor windings are Y-connected. However, the windings connected to the grid are still denoted as stator while the ones connected to the converters as rotor in the following in order to align with the concept. In the setup, the stator (real rotor) of the induction machine is connected to the grid via a variable transformer in order to avoid the high starting current and torque. The rotor (real stator) windings are connected to a back-to-back converter controlled by a dSpace controller box. SPWM is applied to the two converters with the same switching frequency of 2 kHz with a "dead time" of 4 μs. The modulation index for both converters is 0.9.

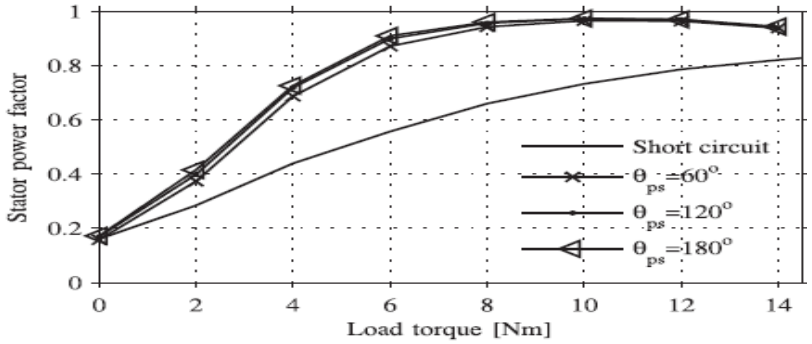

Fig:7. Power factor of induction machine with and without converter.

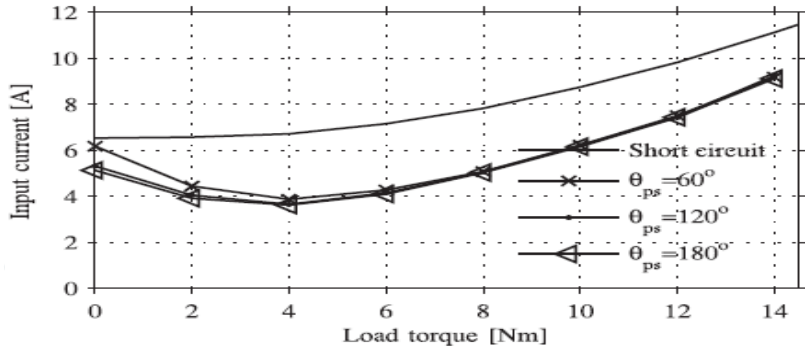

Fig:8. Stator current of induction machine with and without converter.

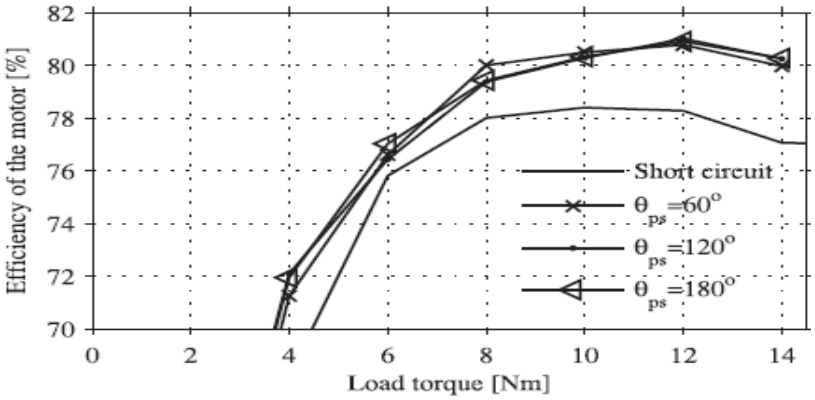

Fig. 9. Efficiency of induction machine with and without converter.

The induction machine is loaded by a dc machine. The field winding of the dc machine is fed by a three-phase rectifier which is supplied by another variable transformer. In addition, a resistor bank is connected to the armature of the dc machine as a resistive load. The speed is measured from a voltage signal proportional to the speed.

IV. POWER FACTOR VERSUS LOAD

Measurement of power factor is presented in this section. The induction machine operating with the rotor-connected converter runs at a constant speed of 1400 r/min while machine operating

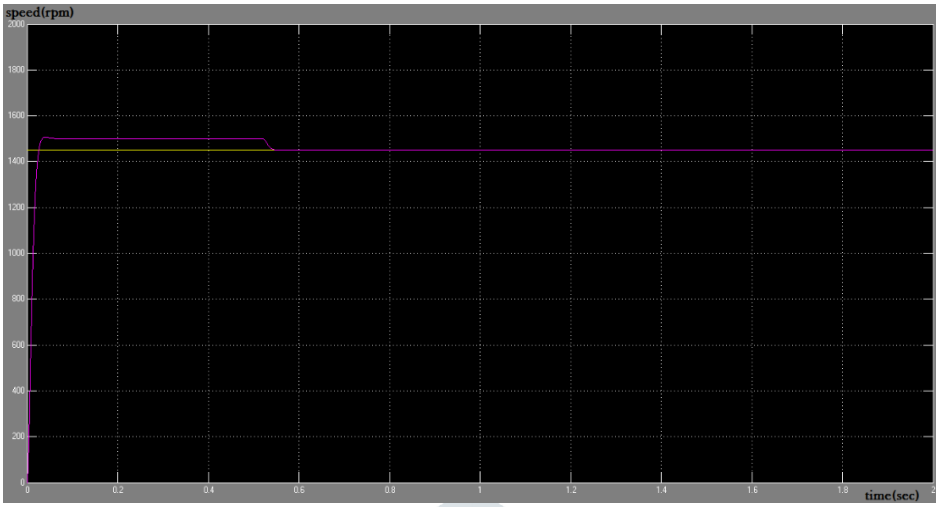

Fig:10. Simulation results for the dynamic performance of the system Speed

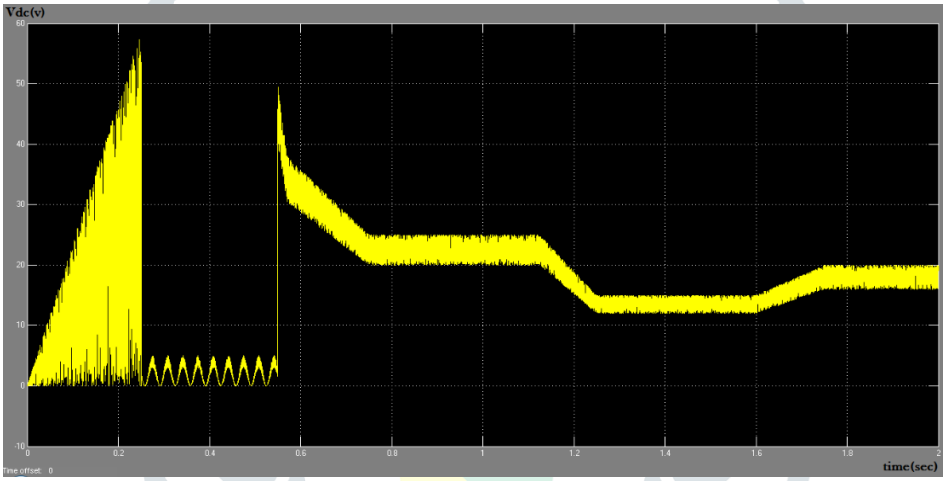

Fig:11. Simulation results for the dynamic performance of the system capacitor voltage

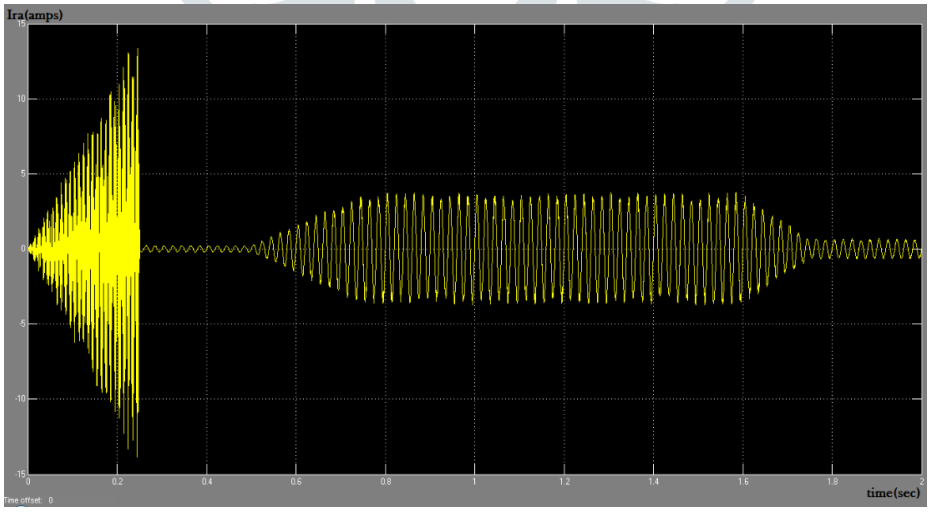

Fig:12. Simulation results for the dynamic performance of the system Rotor current of Phase A

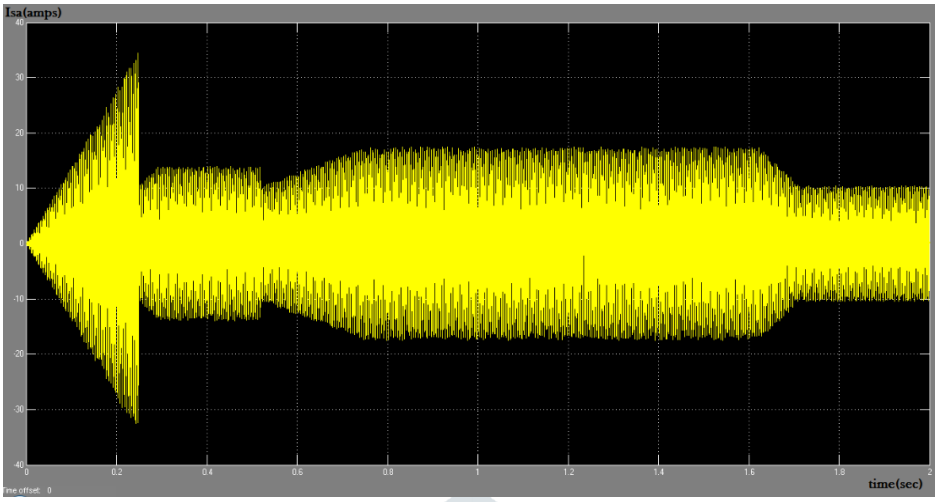

Fig:13. Simulation results for the dynamic performance of the system: Stator current of Phase A.

Without the converter follows its original torque-speed curve, which implies that the speed changes with load. The torque speed relationship of the induction motor without converter can be found in [28].

Fig.7 shows the stator power factor as a function of the load torque for the induction machine with and without converter connected in the rotor. As can be seen, the stator power factor increases with increasing load when the rotor windings are short circuited. Once the back-to-back converter is connected with a non-zero phase-shift angle θps between the two converters, the power factor is effectively improved. Moreover, changing θps has no significant impact on improving the power factor. This can be observed in Fig. 7 when θps is set to 60◦, 120◦ and 180◦, respectively. Furthermore, the required stator current will be reduced as expected since the power factor is improved, as can be seen in Fig. 8. Therefore the copper losses in the stator windings will be reduced thereby improving the efficiency of the machine, as shown in Fig. 9.

Measurements also showed another2%increase in efficiency when the losses in the grid are considered. These losses do not include the losses in the transformer connected between the grid and the motor. Including them would have increased the efficiency even further.

V. DYNAMIC PERFORMANCE OF THE SYSTEM

Dynamic performance of the presented induction machine, including starting, loading and load changing, are investigated through simulation and experiment. The simulated and measured results including speed, capacitor voltage and currents in the rotor and the stator are shown in Figs. 10 and 11, respectively. The reference speed signals is set to 1400 r/min by controlling the fundamental frequency of IGBTs at 3.3 Hz from t = 0 s. A similar starting procedure is applied both in the simulation and experiment.

In the simulation results shown in Fig. 10 the supply voltage is ramped from t = 0s to t = 4s at no load with θps = 60◦. The dc-link capacitor voltage is oscillating during the acceleration and the maximum

value is 57V approximately. The machine accelerates to the no-load speed within around 3 s and stabilizes at the no-load speed without following the reference speed. This is because, as explained in Section II, the capacitor voltage during start-up is unstable and the converter is therefore unable to provide a sufficient voltage at the frequency of 3.33 Hz to the rotor windings. The starting currents in the rotor and stator gradually rise to their maximum values, 16.5 and 34 A(peak), respectively. Note that peak values are used in following if not defined otherwise. When the speed becomes stable, the capacitor voltage declines rapidly and oscillates between 0 and 5 V due to the low no-load rotor current. The rotor current at no load steady state is 0.5A to overcome the friction. The stator current decreases to around 5A when the rotor reaches the no-load speed but gradually rises to 9A as full voltage is applied.

At t = 10 s, the load torque is ramped up from 0 to the rated value of 12.3N·m within 5 s. During this period the rotor current increases and charges the capacitor. At t = 11.4 s the capacitor voltage is increased to its peak value of 49 V and then stabilizes to 25.7 V after t = 15 s. As $\theta ps = 60^{\circ}$, the converter supplies a voltage to the rotor windings. The frequency of the voltage is set to 3.33 Hz thus the speed is synchronized to 1400 r/min at around t = 12s before full load is applied. Meanwhile, the stator current rises at first but has a dip at around t = 11.5 s before it gets stable. The dip can also be seen in the measurements at around t = 13 s in Fig. 11(d).

At t = 22 s, θps is ramped from 60° to 180° in 3 s. The capacitor voltage falls to 13.2 V and keeps oscillating with a ripple of 8 V, while the speed is kept the same. This can be seen in both the simulations and measurements. When the capacitor voltage decreases, the stator current at rated load increases from 11 to 11.8 A which are 77% and 83% of the rated current. This implies the stator power improvement of the induction machine.

At t = 31 s, the load torque is reduced gradually from the rated value to 0. It can be seen that even though the rotor current is decreased, Fig. 10(c), the capacitor voltage increases since the voltage drop on the rotor winding is reduced with the reduced current. In addition, the stator current decreases but rises again to 7.8 A after t = 34s, Fig. 10(d). This no-load current is lower than the current between the period 4–10 s, which is also at no load. This is because the capacitor voltage after t = 34 s is around 20 V and the induction machine is then magnetized from the rotor side. Therefore the required stator current becomes less. Meanwhile it can be noted that the speed of the induction machine is kept the same during the load torque decrease. This implies that the induction machine with the rotor fed by a converter is capable to operate at constant speed and variable load.

In general the experimental results in Fig. 11 show the same trend as the simulation results. There are however some differences. Particularly, the simulated and measured currents at steady state are different. The main reason for this is that the saturation of the machine is not considered in the simulation. In addition, the measured speed signal has some noise. This is because the speed signal is obtained from a voltage signal which corresponds to 1% of the r/min speed of the machine. The speed signal is thus very sensitive to

disturbances. A speed sensor is not used in this setup. The precision of the signal is therefore rather poor. More importantly, it can be seen in Fig. 11(a) that there is no obvious change in the speed after it settles to the demanded value at t = 12 s approximately. It is shown that both simulation and measurement results share the same trend which validates the concept and the dynamic performance.

VI. CONCLUSION

In the presented induction machine with converter-fed rotor windings, the stator power factor can be effectively improved within a wide load range. Correspondingly, the efficiency of the induction machine is increased. The efficiency is further improved considering the losses in the power distribution network. Results for the dynamic performance including starting, loading and deloading of the induction machine are presented from simulation and experiments based on a 1.8kW induction machine with good agreement. It shows that the induction machine is capable of operating at constant speed and variable load by setting the fundamental frequency of the converter. The dc-link capacitor voltage is considerably low which implies a significant reduction of capacitor and converter size.

REFERENCES

[1] S. Das, G. Das, P. Purkait, and S. Chakravorti, "Anomalies in harmonic distortion and Concordia pattern analyses in induction motors due to capacitor bank malfunctions," in *Proc. Int. Power Syst. Conf.*, Dec..27– 29, 2009, pp. 1–6.

[2] R. Spee and A. K. Wallace, "Comparative evaluation of power factor improvement techniques for squirrel cage induction motors," *IEEE Trans. Ind. Appl.*, vol. 28, no. 2, pp. 38–386, Mar./Apr. 1992.

[3] N. H. Malik and A. A. Mazi, "Capacitance requirements for isolated self excited induction generators," *IEEE Trans. Energy Convers.*, vol. EC-2, no. 1, pp. 62–69, Mar. 1987.

[4] M. Ermis, Z. Cakir, I. Cadirci, G. Zenginobuz, and H. Tezcan, "Self excitation of induction motors compensated by permanently connected capacitors and recommendations for IEEE std 141-1993," *IEEE Trans. Ind. Appl.*, vol. 39, no. 2, pp. 313–324, Mar./Apr. 2003.

[5] L. Ruan, W. Zhang, and P. Ye, "Unity power factor operation for three phase induction motor," in *Proc. 3rd Int. Power Electron. Motion Control Conf.*, 2000, vol. 3, pp. 1414–1419.

[6] E. R. Laithwaite and S. B. Kuznetsov, "Cage-rotor induction motor with unity power factor," *IEEE Proc. B Elect. Power Appl.*, vol. 129, no. 3, pp. 143–150, May 1982.

[7] E. R. Laithwaite and S. B. Kuznetsov, "Test results obtained from a brushless unity-power-factor induction machine," *IEEE Trans. Power App. Syst.*, vol. PAS-100, no. 6, pp. 2889–2897, Jun. 1981.

[8] "Discussion on unity-power-factor induction motors," *IEEE Proc. Elect. Power Appl.*, vol. 130, no. 1, pp. 60–68, Jan. 1983.

[9] F. J. T. E. Ferreira and A.T. Almeida, "Novel multiflux level, three phase, squirrel-cage induction motor for efficiency and power factor maximization," *IEEE Trans. Energy Convers.*, vol. 23, no. 1, pp. 101–109, Mar. 2008.

[10] M. V. Aware, S. G. Tarnekar, and A. G. Kothari, "Unity power factor and efficiency control of a voltage source inverter-fed variable-speed induction motor drive," *IEE Proc. Elect. Power Appl.*, vol. 147, no. 5, pp. 422–430, Sep. 2000.